

# Polarization Beam Splitter Based on Self-Collimation of a Hybrid Photonic Crystal

Fulya BAGCI<sup>1</sup>, Sultan CAN<sup>2</sup>, Baris AKAOGLU<sup>1</sup>, A. Egemen YILMAZ<sup>2</sup>

<sup>1</sup> Dept. of Engineering Physics, Ankara University, 06100 Besevler, Ankara, Turkey

<sup>2</sup> Dept. of Electrical-Electronics Engineering, Ankara University, 06830 Golbasi, Ankara, Turkey

fbagci@eng.ankara.edu.tr, sultancan@ankara.edu.tr, akaoglu@eng.ankara.edu.tr, aeyilmaz@eng.ankara.edu.tr

**Abstract.** A photonic crystal polarization beam splitter based on photonic band gap and self-collimation effects is designed for optical communication wavelengths. The photonic crystal structure consists of a polarization-insensitive self-collimation region and a splitting region. TM- and TE-polarized waves propagate without diffraction in the self-collimation region, whereas they split by 90 degrees in the splitting region. Efficiency of more than 75% for TM- and TE-polarized light is obtained for a polarization beam splitter size of only  $17 \mu\text{m} \times 17 \mu\text{m}$  in a wavelength interval of 60 nm including 1.55  $\mu\text{m}$ .

## Keywords

Photonic crystals, self-collimation, photonic band gap

## 1. Introduction

Photonic crystals (PCs) have growing reputation due to their large variety of advantages within ultra-compact sizes [1], [2]. One of the most crucial properties of the PCs is having photonic band gap (PBG) property in which electromagnetic waves cannot propagate in any direction. Light of certain frequencies in a PBG can be guided in a photonic crystal waveguide in the lateral direction by the periodicity of the lattice and in the vertical direction by means of total internal reflection [3]. Besides, the interest to these materials led the researchers to discover new ways to control the flow of light through these structures. Of particular interest is the self-collimation effect, by which the electromagnetic waves can propagate without diffraction in a perfect photonic crystal in the absence of a waveguide. First proposed by Kosaka et al. [4] and promoted by Prather et al. [5] and others [6-10], the phenomenon of self-collimation has been employed in many schemes for a large variety of device applications ranging from bends, splitters, interferometers to filters and detectors. In particular, the self-collimation effect is very preferable for device implementations on-chip integrated photonic circuits due to its arbitrary beam routing efficiency without crosstalk.

In this study, a hybrid photonic crystal consisting of a polarization-independent self-collimation region and a splitting region is employed to achieve polarization splitting. The polarization-independent self-collimation (PIS) region is used to direct the TM- and TE-polarized waves simultaneously without diffraction. The splitting region is formed by changing the composition of the  $\text{Al}_x\text{Ga}_{1-x}\text{As}$  alloy in a rectangular region inside the PIS region, in which the refractive index of that region is changed to be inside the photonic band gap for one of the orthogonal modes. The equi-frequency contours and photonic band diagrams of the PC are obtained with plane-wave expansion (PWE) method, while the field propagation and splitting properties of the device are determined with finite-difference time-domain simulations (FDTD) [11].

## 2. Design and Method

The polarization beam splitter structure presented in this study is illustrated in Fig. 1. It consists of two regions, namely the PIS region and the splitting region. Both of these structures consist of a square lattice of air holes of the same radius in  $\text{Al}_x\text{Ga}_{1-x}\text{As}$  alloy; however with higher refractive index introduced in the splitting region by changing the composition ( $x$ ). When kept in mind that, the special points of the Brillouin zone for a square lattice PC at the center, corner and face are known as  $\Gamma$ , M and X, the splitting region is aligned along the  $\Gamma\text{M}$  direction, whereas light is incident along the  $\Gamma\text{X}$  direction. When the TM- and TE-polarized light reaches the splitting region, the two orthogonal polarizations split by 90 degrees. The TE-polarized light follows the path 1 by virtue of the self-collimation, while the TM-polarized light makes a turn in the direction of path 2 due to the photonic band gap effect (Fig. 1).

In the preliminary calculations, the TM photonic band gap is found to be increasing up to  $r = 0.36a$  and decreasing later as the radius of the holes increases. The radius of air holes is chosen as  $r = 0.36a$ , where  $a$  is the lattice constant so that a better overlap between the self-collimated wavelength region and photonic band gap region is provided. The lattice constant is arranged as 628 nm to render

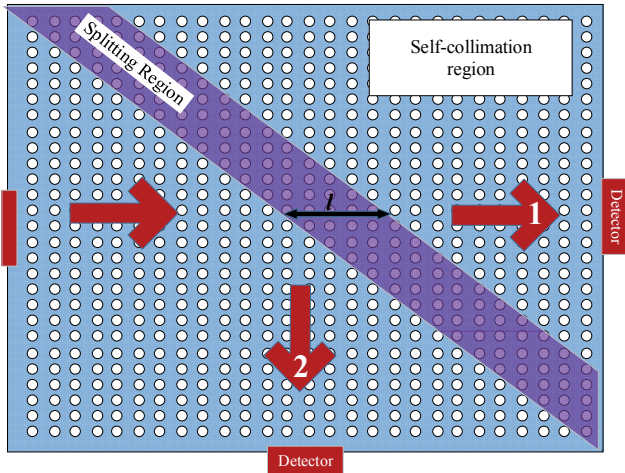


Fig. 1. The geometry of the proposed photonic crystal based polarization beam splitter structure.

the operation wavelength centered at  $1.55 \mu\text{m}$ . Three dimensional PWE and FDTD calculations are approximated in two-dimensions with an effective index value of 2.4 for the PIS region and an effective index value of 2.8 for the splitting region of the PC [12].

### 3. Simulation and Analysis

The contours of constant frequency along the  $k_x$  and  $k_y$  wave-vector plane are called equi-frequency contours (EFCs). The group velocity is the velocity of energy transport and defined by  $\mathcal{S}_G = \nabla_k \omega(k)$ , where  $k$  is the Bloch wave-vector. The group velocity is always perpendicular to the EFCs and it is aligned in the increasing  $\omega(k)$  direction. Light propagates without diffraction in the flat (not curved) regions of the EFC. A mode can be identified by its unique combination  $(k, n)$ , where  $n$  is called the band number in the band diagram. The EFCs of the second ( $n=2$ ) TM (Fig. 2(a)) and TE band (Fig. 2(b)) for the self-collimated PC are square-shaped for the range of normalized frequencies,  $\omega = 0.40(c/a) - 0.42(c/a)$ , for both TM- and TE-polarizations. In these frequencies, polarization independent self-collimation can be observed along the faces of the square-shaped EFCs which are aligned along the  $\Gamma X$  and  $X\Gamma$  direction, as seen in Fig. 2.

Full-width half-maximums of the input and output beams are examined for the two orthogonal polarizations by FDTD simulations in order to verify the self-collimation effect that is predicted by the PWE method. As seen in Fig. 3, no remarkable broadening occurs for TM- and TE-polarized waves in the self collimated PC after propagation along  $31.4 \mu\text{m}$  distance ( $50a$ ).

Once the PIS region of the polarization beam splitter is designed, the properties of the splitting region are investigated in order to achieve the separation of the different polarizations. Fig. 4 shows the photonic band diagram of the splitting region for TM- and TE-modes. As the refractive index of the PC is increased to 2.8 in the

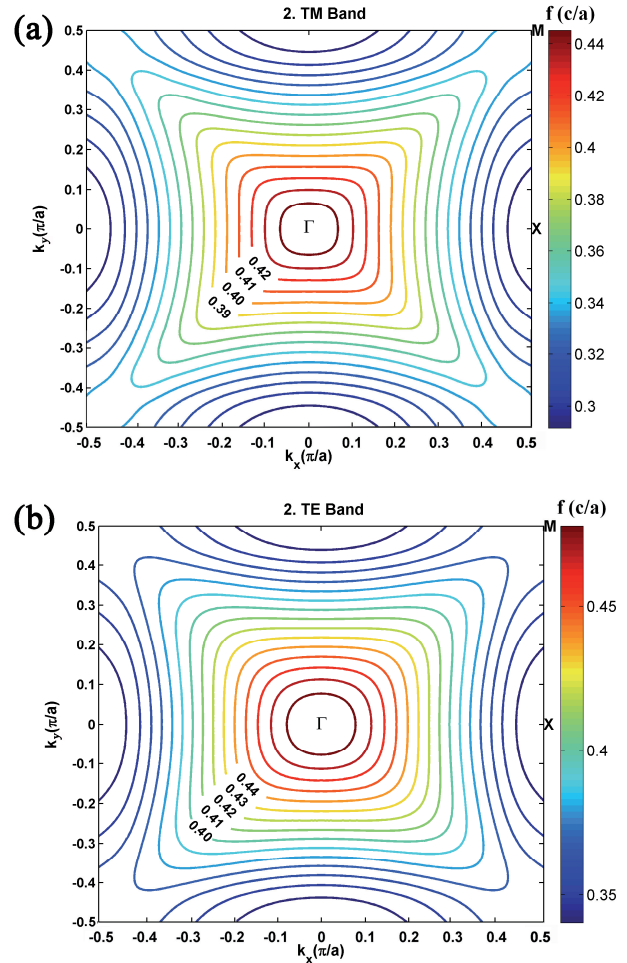


Fig. 2. Equi-frequency contours of the second band for (a) TM modes and (b) TE modes of the self-collimating photonic crystal.

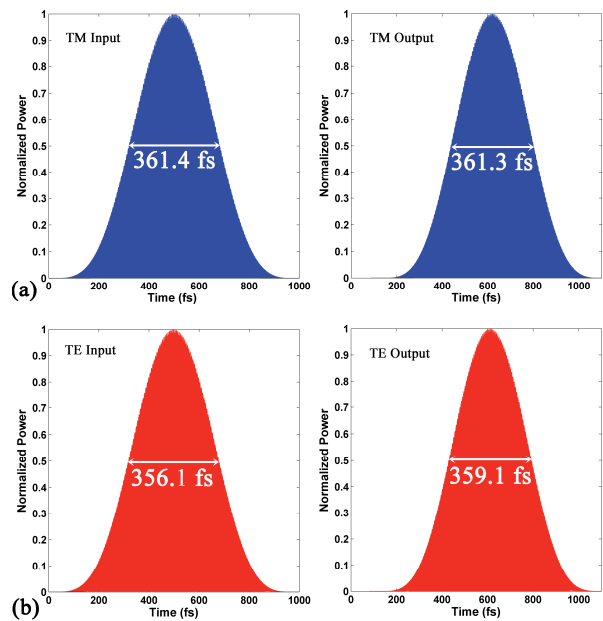


Fig. 3. Time-pulse shapes detected at the input and the output detecting points of the self-collimating photonic crystal for (a) TM modes and (b) TE modes.

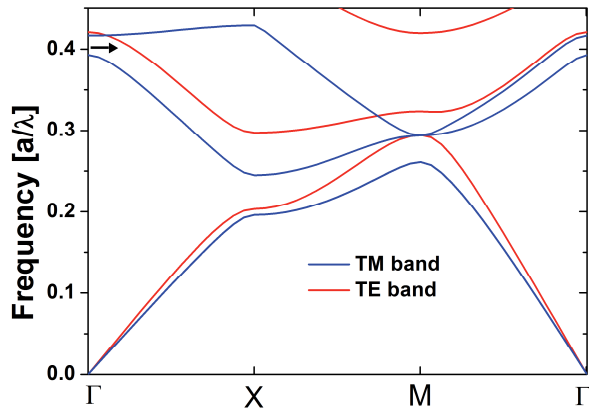


Fig. 4. Band diagram for the splitting region of the photonic crystal with  $n=2.8$ . The small arrow points the operation frequency region of the beam splitter.

splitting region, a photonic band gap appears for the TM-polarized light between the normalized frequencies,  $\omega = 0.39(c/a) - 0.42(c/a)$ . However, since the electric field confines in the air holes for the TE-mode, it is not affected by the refractive index increase as much as the TM-mode. Therefore, there still exists a mode for the TE-polarized waves along the  $\Gamma X$  direction. As the incoming light reaches the splitting region, the TM-polarized waves reflect in the perpendicular direction, whereas the TE-polarized waves propagate directly in the self-collimation regime.

We employ a PC of  $27a \times 27a$  size in order to quantify the transmission and reflection efficiency of the polarization beam splitter through FDTD simulations. The perfectly matched layers of  $2a$  thickness are imposed on the four edges of the PC layer to prevent reflection. The simulation engine [11] uses uniaxial perfectly matched layers [13] by introducing a special lossy anisotropic material which changes both the dielectric constant and magnetic permittivity. A Gaussian source of frequency  $\omega = 0.405(c/a)$  with the full-width half-maximum of 360 fs is launched into the PC along the  $\Gamma X$  direction. Two detectors are placed at the exits of the two ports of the PC as shown in Fig. 1. To obtain the normalized transmission and reflection spectra, the intensity of the transmitted and reflected light beam gathered through these detectors are integrated across the beam cross section and normalized with respect to the incident beam. An abrupt change of refractive index in the splitting region is observed to cause high level of reflection and refraction loss. To minimize the leakage along the boundary between the PIS and the splitting region, a gradual refractive index change is employed through the edges of the splitting region. This is accomplished by inserting three layers of regions with widths of  $1.5a$ ,  $2a$  and  $1.5a$  inside the PC side by side as the splitting region. From the refractive index of 2.4 to 2.8 the refractive index is increased linearly in the first PC layer, from the refractive index of 2.8 to 2.4 the refractive index is decreased linearly in the third PC layer; whereas the refractive index is fixed to 2.8 in the middle PC layer. Graded refractive index materials are often employed in anti-reflection coatings, light-emitting diodes and solar

cells to eliminate Fresnel reflection by fabricating coatings whose refractive index gradually changes from the refractive index of the active semiconductor layer to the refractive index of the surrounding medium [14-16].

It can be seen at Fig. 5 that the reflection of the TM-polarized light is above 75 % between  $1.53 \mu\text{m}$  and  $1.59 \mu\text{m}$  and the transmission of TE-polarized light is above 85 % in the 80 nm operation bandwidth of the polarization beam splitter. A transmission of 93 % for TE-polarized light and reflection of 79.5 % for TM-polarized light are obtained at  $1.55 \mu\text{m}$ . In one of the studies on PC polarization beam splitter, a PC beam splitter is designed by changing the filling fraction of the PC in the splitting region, while maintaining the lattice constant and radius of the holes of the PC [8]. The simulations are realized in 2Ds with an effective index and up to 83 % transmission/reflection for TM/TE polarizations are achieved. Here, we obtain higher reflection and transmission ratios by applying a novel method, i.e. tuning the refractive index of the splitting region locally in the PIS region.

The polarization extinction ratios (PERs) of the transmitted and reflected beams are defined as  $-10\log(T_{\text{TM}}/T_{\text{TE}})$  and  $-10\log(R_{\text{TE}}/R_{\text{TM}})$ , respectively. The PERs of the transmitted and reflected beams at  $1.55 \mu\text{m}$  wavelength are calculated as 12.7 dB and 18.3 dB, respectively. Recently, a PC polarization beam splitter based on a self-collimated Michelson interferometer is demonstrated in silicon by using two beam splitters and four mirrors in a large Si PC [17]. The calculations are performed in 2Ds without scaling down the thickness of the Si slab by using an effective index. Although higher PER values are obtained (18.4 dB for TM and 24.3 dB for TE mode) in that study, these values are only valid for the optimized fixed single frequency value and decrease immediately in the surrounding frequencies due to the destructive interference nature of the Michelson interferometer.

As the splitting region, Chen et al. [18] used an air block that is aligned along the  $\Gamma M$  direction inside a Si PC lattice of holes to divide the TE- and TM-polarized waves simultaneously through the two ports. A maximum efficiency of 48 % for TE-polarization at an air block width of  $0.18a$  and 49.9 % for TM-polarization at an air block width of  $0.33a$  are obtained [18]. Although the production is simple, the width of the air block is critical for achieving maximum efficiency of the splitter in that study. However, since the refractive index of the splitting region is tuned smoothly in our study, the transmission efficiency does not show such an abrupt change. The size of the splitting region can be a little increased to enhance the TM reflection ratio at the cost of a modest decrease in the TE transmission. For example, when the width of the splitting region in the middle PC layer is increased to  $3a$ , the maximum transmission and reflection efficiencies are 84 % and 87 % for TE- and TM-polarized light, respectively.

The FDTD simulation of the light propagation through the proposed PC based polarization splitting structure is illustrated in Fig. 6. It can be seen that the TE-

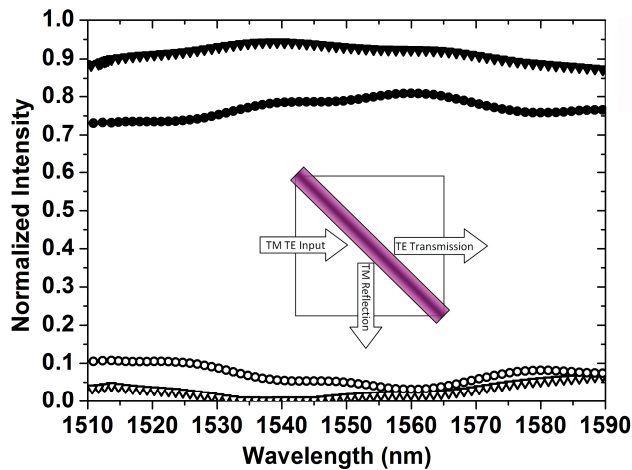


Fig. 5. The transmission of TE ( $\nabla$ ), TM ( $\circ$ ) and the reflection of TE ( $\nabla$ ) and TM ( $\bullet$ ) polarized light beams against the incident self-collimated light.

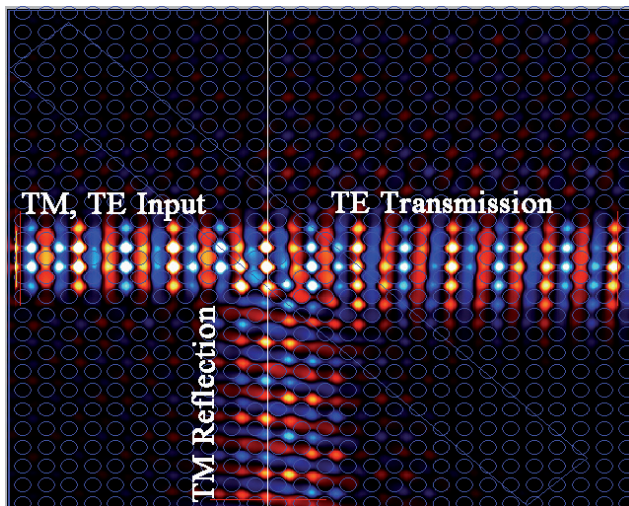


Fig. 6. Simulation of the light propagation through the photonic crystal based polarization beam splitter.

polarized light beams transmit directly and the TM-polarized light beams make a 90 degree turn after passing through the splitting region, with the maintenance of the self-collimation ability.

## 4. Conclusions

We have proposed and numerically demonstrated a photonic crystal based polarization beam splitter with high splitting efficiency, large separation angle and low crosstalk at the optical communication wavelengths. The transmission and reflection efficiencies of the device for TE and TM polarizations are found to be 93 % and 79.5 %, respectively at 1.55  $\mu\text{m}$ . Moreover the efficiencies stay above 70 % for both polarizations between 1.51  $\mu\text{m}$  and 1.59  $\mu\text{m}$ . The proposed device can be very useful in optical devices and integrated photonic circuits, where polarization insensitivity is needed. For example, it can be used in photonic system-on-chip applications with other photonic components such as light emitters, waveguides, resonators, etc.

## Acknowledgements

We gratefully acknowledge the financial support by Scientific Research Projects of Ankara University (BAP) under Grant no. 13B4343015.

## References

- [1] YABLONOVITCH, E. Inhibited spontaneous emission in solid state physics and electronics. *Physical Review Letters*, 1987, vol. 58, p. 2059–2062.
- [2] JOANNOPOULOS, J. D., MEADE, R. D., WINN, J. N. *Photonic Crystals: Molding the Flow of Light*. 2<sup>nd</sup> ed. NJ: Princeton, 2008.
- [3] JOHNSON, S. G., FAN, S. H., VILLENEUVE, P. R., JOANNOPOULOS, J. D., KOLODZIEJSKI, L. Guided modes in photonic crystal slabs. *Physical Review B*, 1999, vol. 60, p. 5751 to 5758.
- [4] KOSAKA, H., KAWASHIMA, T., TOMITA, A., NOTOMI, M., TAMAMURA, T., SATO, T., KAWAKAMI, S. Self-collimating phenomena in photonic crystals. *Applied Physics Letters*, 1999, vol. 74, no. 9, p. 1212–1214.
- [5] PRATHER, D. W., SHI, S., MURAKOWSKI, J., SCHNEIDER, G. J., SHARKAWY, A., CHEN, C., MIAO, B., MARTIN, R. Self-collimation in photonic crystal structures: a new paradigm for applications and device development. *Journal of Physics D: Applied Physics*, 2007, vol. 40, no. 9, p. 2635–2651.
- [6] YU, X., FAN, S. Bends and splitters for self-collimated beams in photonic crystal. *Applied Physics Letters*, 2003, vol. 83, no. 16, p. 3251–3253.
- [7] ZHAO, D., ZHANG, J., YAO, P., JIANG, X., CHEN, X. Photonic crystal Mach-Zehnder interferometer based on selfcollimation. *Applied Physics Letters*, 2007, vol. 90, no. 23, p. 231114.
- [8] ZABELIN, V., DUNBAR, L. A., THOMAS, N. Le, HOUDRE, R., KOTLYAR, M. V., O'FAOLAIN, L., KRAUSS, T. F. Self-collimating photonic crystal polarization beam splitter. *Optics Letters*, 2009, vol. 17, no. 22, p. 19808–19813.
- [9] CHEN, X., QIANG, Z., ZHAO, D., LI, H., QUI, Y., YANG, W., ZHOU, W. Polarization-independent drop filters based on photonic crystal self-collimation ring resonators. *Optics Express*, 2009, vol. 17, no. 22, p. 19808–19813.
- [10] KIM, T. T., LEE, S. G., PARK, H. Y., KIM, J. E., KEE, C. S. Asymmetric Mach-Zehnder filter based on self-collimation phenomenon in two-dimensional photonic crystals. *Optics Express*, 2010, vol. 18, no. 6, p. 5384–5389.
- [11] CrystalWave from Photon Design. Available at: <http://www.photond.com>.
- [12] QUI, M. Effective index method for heterostructure-slab-waveguide-based two dimensional photonic crystals. *Applied Physics Letters*, 2002, vol. 81, p. 1163–1165.
- [13] GEDNEY, S. D. An anisotropic perfectly matched layer absorbing media for the truncation of FDTD lattices. *IEEE Transactions on Antennas and Propagation*, 1996, vol. 44, no. 12, p. 1630–1639.
- [14] SOUTHWELL, W. H. Gradient-index antireflection coatings. *Optics Letters*, 1983, vol. 8, no. 11, p. 584–586.
- [15] KIM, J. K., CHHAJED, S., SCHUBERT, M. F., SCHUBERT, E. F., FISCHER, A. J., CRAWFORD, M. H., CHO, J., KIM, H., SONE, C. Light-extraction enhancement of GaInN light-emitting diodes by graded-refractive-index indium tin oxide anti-reflection contact. *Advanced Materials*, 2008, vol. 20, no. 4, p. 801–804.

- [16] ZHAO, Y., CHEN, F., SHEN, Q., ZHANG, L. Optimal design of light trapping in thin-film solar cells enhanced with graded  $\text{SiN}_x$  and  $\text{SiO}_x\text{N}_y$  structure. *Optics Express*, 2012, vol. 20, no. 10, p. 11121-11136.
- [17] CHEN, X.-Y., LIN, G.-M., LI, J.J., XU, X.F., JIANG, J.Z., QIANG, Z.-X., QUI, Y.S., LI, H. Polarization beam splitter based on a self-collimation Michelson interferometer in a silicon photonic crystal. *Chinese Physics Letters*, 2012, vol. 29, no. 1, p. 014210-1-4.
- [18] SHEN, X., HAN, K., YANG, X., SHEN, Y., LI, H., TANG, G., GUO, Z. Polarization-independent self-collimating bends and beam splitters in photonic crystals. *Chinese Optics Letters*, 2007, vol. 5, no. 11, p. 662-664.

### About Authors ...

**Fulya BAGCI** obtained her first degree in Engineering Physics from Ankara University, graduating in 2005. She received her M.Sc. and Ph.D. degrees from the same university in 2008 and 2013, respectively. Dr. Bagci is a research assistant in the Department of Engineering Physics, Ankara University since 2005. Her current research interests include the analysis of photonic crystals and metamaterials for photonic and microwave device applications.

**Sultan CAN** received her B.Sc. degree in Electrical-Electronics Engineering from the Atilim University in 2008.

She received her M. Sc. degree from the same university in 2011. She is now a Ph.D. candidate in Electrical-Electronics Engineering. She is currently with the Dept. of Electrical-Electronics Engineering in Ankara University, where she is a research assistant. Her research interests include electromagnetism, metamaterials and antennas.

**Baris AKAOGLU** received his B.Sc. degree in Physics from the Middle East Technical University in 1996. He received his M.Sc. and Ph.D. degrees in Physics from the same university in 1998 and 2004, respectively. He is currently with the Dept. of Engineering Physics in Ankara University, where he is an Associated Professor. He did experimental research on semiconductors. His current research interests include photonic crystals and metamaterials.

**Asim Egemen YILMAZ** received his B.Sc. degrees in Electrical-Electronics Engineering and Mathematics from the Middle East Technical University in 1997. He received his M.Sc. and Ph.D. degrees in Electrical-Electronics Engineering from the same university in 2000 and 2007, respectively. He is currently with the Dept. of Electrical-Electronics Engineering in Ankara University, where he is an Associated Professor. His research interests include computational electromagnetics, nature-inspired optimization algorithms, knowledge-based systems; more generally software development processes and methodologies.